Advanced Composite Materials
Publication details, including instructions for authors and subscription information:
http://www.tandfonline.com/loi/tacm20

Chain Extension Effects of para-Phenylene Diisocyanate on Crystallization Behavior and Biodegradability of Poly(lactic acid)/Poly(butylene terephthalate) Blends

Myung Wook Kim [a], Sung Min Hong [b], Doojin Lee [c], Kwangseok Park [d], Tae Jin Kang [e] & Jae Ryoun Youn [f]

[a] Research Institute of Advanced Materials (RIAM), Department of Materials Science and Engineering, Seoul National University, Shinlim-Dong, Gwanak-Gu, Seoul, 151-744, Korea

[b] Advanced Polymeric Materials R&D Center, Samyang Corporation, Hwaam-Dong, Yuseong-Gu, Daejeon, 305-717, Korea

[c] Research Institute of Advanced Materials (RIAM), Department of Materials Science and Engineering, Seoul National University, Shinlim-Dong, Gwanak-Gu, Seoul, 151-744, Korea

[d] Research Institute of Advanced Materials (RIAM), Department of Materials Science and Engineering, Seoul National University, Shinlim-Dong, Gwanak-Gu, Seoul, 151-744, Korea

[e] Research Institute of Advanced Materials (RIAM), Department of Materials Science and Engineering, Seoul National University, Shinlim-Dong, Gwanak-Gu, Seoul, 151-744, Korea

[f] Research Institute of Advanced Materials (RIAM), Department of Materials Science and Engineering, Seoul National University, Shinlim-Dong, Gwanak-Gu, Seoul, 151-744, Korea

Version of record first published: 02 Apr 2012.

VSP

Advanced Composite Materials 19 (2010) 331–348

ADVANCED COMPOSITE MATERIALS
brill.nl/acm

Chain Extension Effects of para-Phenylene Diisocyanate on Crystallization Behavior and Biodegradability of Poly(lactic acid)/Poly(butylene terephthalate) Blends

Myung Wook Kim [a], **Sung Min Hong** [b], **Doojin Lee** [a], **Kwangseok Park** [a], **Tae Jin Kang** [a] **and Jae Ryoun Youn** [a,*]

[a] Research Institute of Advanced Materials (RIAM), Department of Materials Science and Engineering, Seoul National University, Shinlim-Dong, Gwanak-Gu, Seoul, 151-744, Korea
[b] Advanced Polymeric Materials R&D Center, Samyang Corporation, Hwaam-Dong, Yuseong-Gu, Daejeon, 305-717, Korea

Received 8 July 2009; accepted 8 September 2009

Abstract
The blends of poly(lactic acid) (PLA) and poly(butylene terephthalate) (PBT) were prepared with para-phenylene diisocyanate (PPDI) through reaction extrusion. The crystallization behavior of the PLA/PBT blends was investigated by using a differential scanning calorimeter (DSC), a wide angle X-ray diffractometer (WAXD) and a contact angle goniometer. The biodegradability was evaluated with a buffer solution containing esterase. The addition of PBT into a PLA polymer matrix induced the cold crystallization of the PLA phase. The crystallization rate of the PLA phase was accelerated significantly when both PBT and PPDI reacted with PLA simultaneously. But the chain extension caused by PPDI decreased the crystallinity of PLA and PBT phases. The phase separation between PLA and PBT in PLA/PBT blends increased the interfacial area exposed to hydrolysis, resulting in the improved degradability of the PLA phase. In contrast, the improved interfacial adhesion between PLA and PBT caused by the reaction with PPDI reduced the area that was exposed to enzyme and the degradation rate of the PLA phase.

Keywords
Poly(lactic acid), poly(butylene terephthalate), diisocyanate, crystallization, biodegradability

1. Introduction

Biomass polymers have received much attention recently because they have the possibility of solving environmental problems, such as the regulation of carbon dioxide (CO_2) emissions and the exhaustion of fossil fuel [1–5]. PLA has become an im-

* To whom correspondence should be addressed. E-mail: jaeryoun@snu.ac.kr
Translated paper originally published in the Journal of The Korean Society for Composite Materials. Edited by the KSCM

 DOI:10.1163/092430409X12605406698471

portant biomass plastic because it is being commercially produced on a large scale at a reasonable price and possesses high modulus, thermal plasticity, biodegradability and biocompatibility [1–3]. PLA has been used for grocery packages, waste composting bags, sutures, bone fracture fixtures and drug delivery systems [2, 3, 6]. But it is not yet suitable for automotive parts or electrical appliances owing to its disadvantages, such as brittleness, low heat resistance, and poor processability compared with petroleum-based plastics [7]. The heat deflection temperature (HDT) of molded PLA articles is known to be around the glass transition temperature (T_g) of about 57°C because the crystallinity is very low under practical molding conditions due to the slow crystallization rate [8, 9]. The poor processability is also attributed to the slow crystallization rate [8]. In contrast, PBT shows a rapid crystallization rate, excellent processability, and good mechanical properties [10, 11].

PLA has been blended with many polymers, including polycaprolactone, poly(vinyl acetate), poly(butylene adipate-co-terephthalate) (PBAT), poly(ethylene glycol), poly(butylene succinate), hexanoyl chitosan (H-chitosan), polyethylene, etc. to investigate and improve their various properties [7, 12–21]. Jiang *et al.* [13] found that the addition of PBAT accelerated the crystallization rate of PLA but had little effect on its final degree of crystallinity. Peesan *et al*. [16] reported that the crystallinity of a PLA phase in the PLA/H-chitosan blends was monotonically decreased with H-chitosan content.

Meanwhile, it is well known that the biodegradability of PLA depends on its crystallinity, molecular structure and morphology significantly [21]. Li and Yang [2] studied the relationships between the hydrophilicity and biodegradability of PLA reacted with methylene diphenyl diisocyanate (MDI). It was indicated that the degradation rate of PLA increases with the hydrophilicity of the specimens because the hydrolysis of ester bonds occurs on the surface of the specimen. According to Wang *et al*. [22], it was revealed that the interfacial adhesion between PLA and starch phases in PLA/starch blends reacted with MDI was improved by the formation of block copolymers due to the MDI acting as a coupling agent. Lee and Wang [23] investigated the effects of lysine-based diisocyanate (LDI) as a coupling agent on the biodegradability of PLA and bamboo fiber (BF) composites. It was found that the addition of LDI delayed the enzymatic degradation of the PLA/BF composites because the interfacial adhesion between the PLA and the BF improved by the coupling effect of the LDI might decrease the area exposed to the hydrolysis of enzyme.

The effects of PBT having a rapid crystallization rate and PPDI as a chain extender on the crystallization behavior and biodegradability of PLA in PLA/PBT blends were investigated in this study. If they accelerate the crystallization rate of PLA phases in the PLA/PBT blends, the heat resistance of the PLA/PBT blends will be greatly improved under general molding conditions.

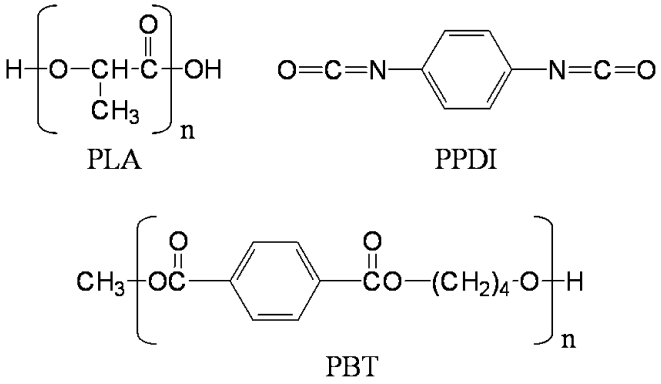

Figure 1. Chemical structures of PLA, PPDI and PBT used in this study.

2. Experimental

2.1. Materials and Sample Preparation

Commercially available PLA (PLA Polymer 4032D, Natureworks LLC) and PBT (TRIBIT 1300, Samyang Co.) resins were used as polymer matrices. The density of the PLA and the PBT was 1.25 and 1.31 g/cm^3, respectively. The number averaged molecular weight, weight averaged molecular weight, and molecular weight distribution of the PLA were 116 300, 206 700 and 1.78, respectively, as estimated by gel permeation chromatography (GPC, 150C, Waters) with chloroform as a solvent. The intrinsic viscosity of the PBT was 0.70 dl/g and PPDI (BASF Co.) was used as a chain extender between PLA and PBT. As the chemical structures of PLA, PPDI, and PBT used in this study, shown in Fig. 1, indicate, the PLA has hydroxyl and carboxyl end groups. The PBT has hydroxyl and methyl ester end groups because it was produced by a dimethyl terephthalate-based batch process. Therefore, it is expected that the isocyanate end groups of the PPDI will react easily with the hydroxyl and carboxyl end groups to extend or connect the chains of PLA and PBT.

PLA/PBT blends were prepared with PPDI by using a co-rotating twin-screw extruder (ZSK-25, Werner and Pfleiderer, diameter = 25 mm, length/diameter = 40) at a melt temperature of 230–240°C, a screw speed of 200 rpm, and a feed rate of 12 kg/h. The extrudate was quenched in a water bath at 20°C and pelletized. The compositions of the prepared samples are listed in Table 1. The specimens for the measurement of HDTs and water contact angles were prepared with an injection molding machine (LGH 100N, LS Cable) at a barrel temperature of 240°C, a mold temperature of 30°C, and a cycle time of approximately 40 s.

2.2. Characterization

The HDTs of unannealed or annealed PLA were compared by using a HDT Tester (6M-2, Toyoseiki). The specimens had a dimension of 127 × 12.7 × 6.4 mm^3, and the HDT was measured with a load of 4.6 kg$_f$/cm^2 at a heating rate of 2°C/min following ASTM D648. The rheological properties were measured at 240°C by using

Table 1.
Compositions of PLA/PBT blends

Sample	Composition (wt%)		
	PLA	PBT	PPDI
PLA	100	–	–
PLA/PBT	50	50	–
PBT	–	100	–
PLA/PPDI	97	–	3
PLA/PBT/PPDI	48.5	48.5	3
PBT/PPDI	–	97	3

a dynamic mechanical rheometer (ARES, Rheometrics) equipped with the parallel-plate geometry of a diameter of 20 mm in order to evaluate the chain extension of PLA/PPDI and PBT/PPDI.

The thermal properties of the samples were investigated under nitrogen by using a DSC (DSC-7, Perkin-Elmer). Two scanning rates of 20 and 10°C/min were applied to examine the effect of cooling and heating rates on the crystallization behaviors of PLA and PBT phases in the PLA/PBT blends. The test samples were heated from 30 to 250°C at a rate of 20 or 10°C/min and held for 5 min at 250°C to eliminate any thermal history. They were then cooled to 30°C at a rate of 20 or 10°C/min and held for 5 min at 30°C. Thereafter, they were reheated to 250°C at a rate of 20 or 10°C/min. The T_g, the crystallization temperature (T_c), and the melting temperature (T_m) were obtained from the DSC curves.

The crystalline properties were analyzed by using a WAXD (AUX D8 advance with GADDS, 40 kV, 40 mA, Cu-K_α, Bruker) at room temperature. The wavelength was 0.1541 nm, and the scattering angle (2θ) ranged from 5° to 90° at a scanning rate of 0.01°/s. The test pellets were annealed at 75°C for 30 min as a precondition to compare the relative crystallization behaviors at a specific temperature of 75°C. The pellets were pulverized into powder under liquid nitrogen by using a freezer mill to prevent the further crystallization of PLA phases in the PLA/PBT blends. The degree of the relative crystallinity was calculated from the diffracted intensity data of the powder by area integration method from the following equation [24–26]:

$$\text{Crystallinity } (\%) = \frac{C}{A + C} \times 100, \tag{1}$$

where A is the area under the amorphous region and C is the area corresponding to the crystalline region.

The surfaces of the PLA/PBT specimens which were annealed at 75°C for 30 min were observed by using a field emission scanning electron microscope (FE-SEM, SUPRA 55VP, Carl Zeiss) after they had been fractured at 15°C. For hydrophilicity measurements, the water contact angles of the specimens annealed at 75°C

for 30 min were determined by using a contact angle goniometer (Phoenix 300, SEO Co.).

Rectangular plates ($12 \times 7.2 \times 1.3$ mm^3) were prepared by compression molding at 240°C for biodegradability measurements and quenched in water at 20°C to prevent the crystallization of PLA phases in the PLA/PBT blends. Thereafter, they were annealed at 75°C for 30 min to reveal the effects of crystallinity, morphology, and hydrophilicity on the biodegradability of the PLA phases with the same annealing condition. Each specimen was immersed in 5 ml of pH 8.0 buffer solution containing esterase (from hog liver, lyophilized, 220 units/mg, Sigma-Aldrich) of 90 units (0.409 mg) at 25°C. The enzyme solution was replenished every 3 days. At a specific period the specimens were retrieved from the enzyme solution and washed by sonication in distilled water for 30 min. They were then weighed after drying in a vacuum oven at 40°C for 24 h.

3. Results and Discussion

3.1. Annealing Effect on the HDT of PLA

Pure PLA is crystallized near 120°C [9, 13, 27]. The HDTs of unannealed PLA and PLA annealed at 120°C for 1 h were measured to investigate the effect of crystallization on the thermal resistance of the pure PLA as shown in Fig. 2. Since the pure PLA was considerably crystallized during annealing at 120°C for 1 h, the HDT was significantly increased from 57.6°C to 132.5°C. Therefore, the crystallization of PLA can be considered as an important factor influencing the thermal resistivity of PLA.

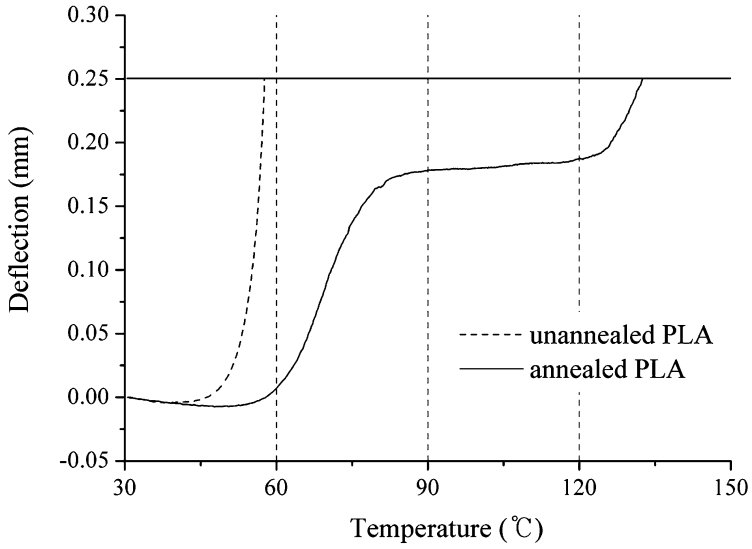

Figure 2. Traces of HDT with a load condition of 4.6 kg$_f$/cm^2 at a heating rate of 2°C/min for unannealed PLA and PLA annealed at 120°C for 1 h.

3.2. Chain Extending

PBT having a fast crystallization rate and PPDI as a chain extender were introduced into a PLA/PBT blending system to improve the crystallization rate of a PLA phase. Figure 3(a) shows the complex viscosities of the PLA and the PBT at 240°C before and after the reaction with the PPDI. The complex viscosities of PLA/PPDI and PBT/PPDI were increased as compared with those of the pure PLA and PBT,

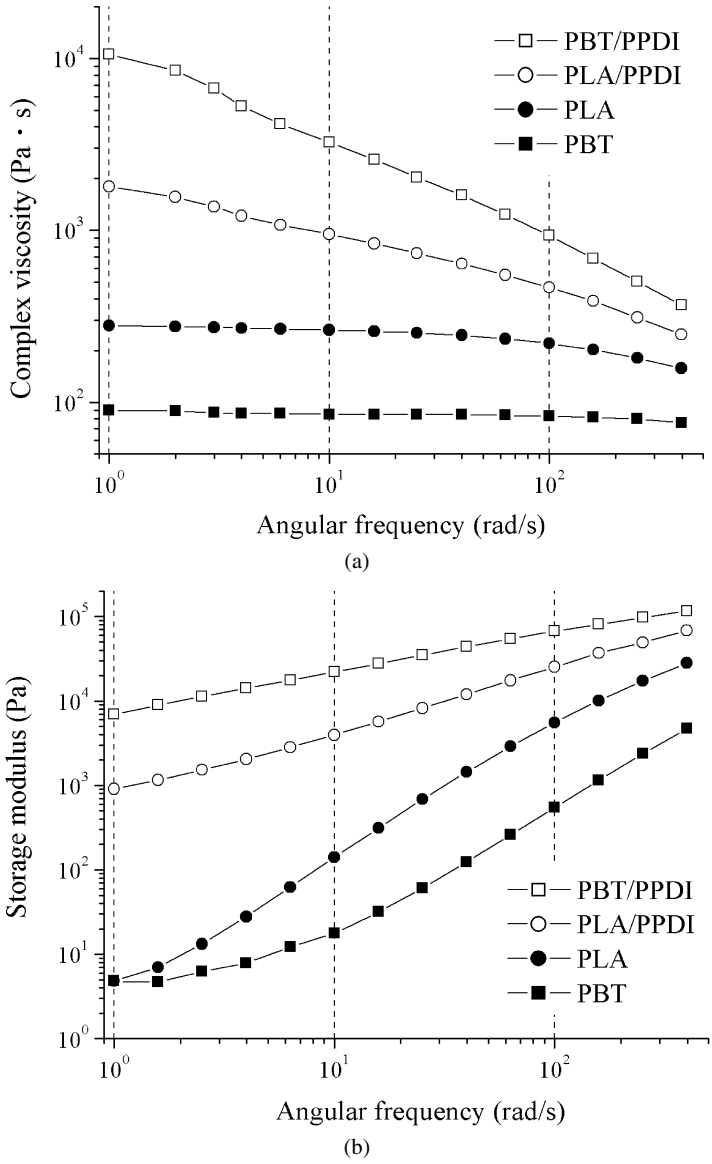

Figure 3. (a) Complex viscosities and (b) storage moduli of the PLA and the PBT at 240°C before and after the reaction with the PPDI.

respectively. Moreover, the shear thinning phenomena of the PLA/PPDI and the PBT/PPDI were observed conspicuously even at low shear rate region. It is well known that shear thinning behavior dominates when molecular weight distribution was broad or molecular structure was branched [28]. Therefore, it is considered that the molecular weights of the PLA and the PBT were increased because the end groups of their molecules could be extended or connected with each other by the PPDI during the reaction extrusion. Their molecules might also be branched by an allophanate reaction caused by incorporating the excess PPDI into the reaction [29, 30]. The PPDI reacted with the PBT more than the PLA in the same extrusion condition because the viscosity of the PBT/PPDI was increased more than that of the PLA/PPDI. The degree of the reaction may be different due to the factor that the PBT has more end groups than the PLA in the same weight because the molecular weight of the PBT is smaller than that of the PLA.

The storage moduli of the pure PLA and PBT were increased and the slopes were decreased after the reaction with PPDI as shown in Fig. 3(b). Therefore, the viscous effects of the polymeric melt were diminished, but the elastic effects were increased due to the increased molecular weight and a chain branching effect. Figure 4 represents the anticipated reactions of chain extension among PLA, PBT and

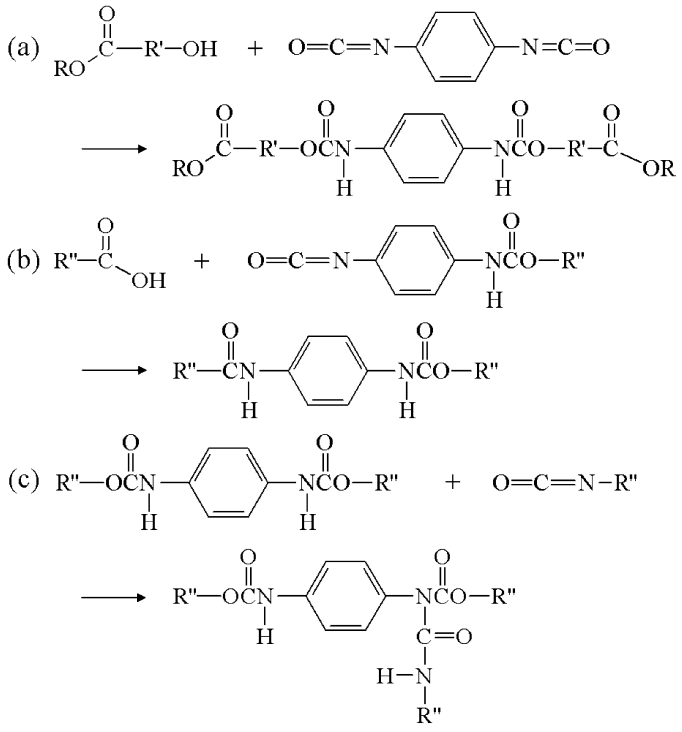

Figure 4. Anticipated reactions of chain extension among PLA, PBT and PPDI with the formation of (a) urethane bonds, (b) amide bonds and (c) allophanate bonds. R is H or CH_3, R′ is the repeating unit of PLA or PBT and R″ represents the bonds reacted among PLA, PBT and PPDI.

PPDI with the formation of urethane bonds, amide bonds and allophanate bonds. The isocyanate end groups of PPDI can be connected with the hydroxyl end groups of PLA or PBT molecules through urethane bonds. An excess amount of the isocyanate groups may also form amide bonds or react with urethane bonds by an allophanate reaction to induce chain branching or cross-linking, which will broaden the molecular weight distribution of the PLA and the PBT [29, 30].

3.3. Crystallization Behavior

Figure 5(a) shows the crystallization behavior of the PLA/PBT melt obtained by the DSC at a cooling rate of 20°C/min. The peaks were generated in the range

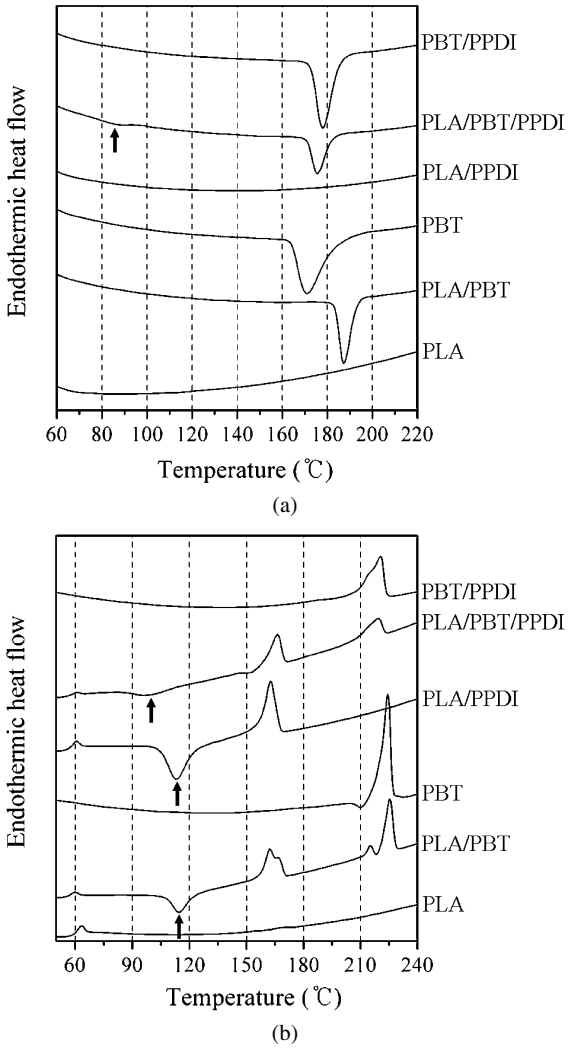

Figure 5. DSC traces of the PLA/PBT blends during (a) a cooling stage and (b) a reheating stage at a rate of 20°C/min.

Table 2.
Thermal properties of the PLA/PBT blends at 20°C/min during a cooling stage

Sample	PLA phase		PBT phase	
	T_c (°C)	ΔH_c (J/g)	T_c (°C)	ΔH_c (J/g)
PLA	–	–	–	–
PLA/PBT	–	–	187.9	23.1
PBT	–	–	171.3	48.9
PLA/PPDI	–	–	–	–
PLA/PBT/PPDI	85.9	3.0	175.9	17.1
PBT/PPDI	–	–	178.3	35.3

of 160–200°C by the crystallization of the PBT phase. The crystallization temperature and enthalpy of the PLA/PBT blends during a cooling stage are listed in Table 2. The incorporation of PLA or PPDI into PBT matrix increased the crystallization temperature of the PBT by about 9°C. The crystallization peak of the PLA phases was not found except for PLA/PBT/PPDI. The PLA crystallization peak of the PLA/PBT/PPDI observed near 86°C indicates that the crystallization rate of the PLA phase was accelerated in the PLA/PBT/PPDI.

Figure 5(b) compares the crystallization and melting properties of the PLA/PBT blends at a reheating rate of 20°C/min. In the case of pure PLA, only the T_g was detected, but there was no melting peak since the crystallization of the PLA did not take place during the DSC analysis. The melting peaks of PLA and PBT phases were observed near 165°C and 220°C, respectively. The PBT crystallization peaks were not detected because the crystallization of the PBT phase had been completed at a cooling rate of 20°C/min. In the case of PLA/PBT, a melting peak and a shoulder in the PLA phase were separated near 165°C and two melting peaks in the PBT phase were observed near 220°C. This may indicate that a new crystalline structure was induced by blending PLA and PBT. However, the bimodal melting peak may also be induced due to the annealing effect occurring during the slow DSC scan if the less perfect crystals had enough time to melt and be transformed into more perfect crystals, then remelted at higher temperature [13, 31]. Thus, the change in the crystalline structure was further investigated through the analysis of WAXD.

The addition of PBT or PPDI into PLA matrix induced the cold crystallization of a PLA phase at 114°C, and the cold crystallization peak of the PLA phase in the PLA/PBT/PPDI was observed at 99°C during the reheating stage. The lower cold crystallization temperature (T_{cc}) in a heating step means that the crystallization happens earlier in the same condition. Therefore, the crystallization rate of a PLA phase can be greatly increased when both PBT and PPDI are added simultaneously into a PLA/PBT blending system, like the DSC results during the cooling stage. The thermal and crystalline properties of the PLA/PBT blends during the reheating

Table 3.
Thermal and crystalline properties of the PLA/PBT blends at 20°C/min during a reheating stage

Sample	PLA phase					PBT phase	
	T_g (°C)	T_{cc} (°C)	ΔH_{cc} (J/g)	T_m (°C)	X_c (%)	T_m (°C)	X_c (%)
PLA	59.2	–	–	–	0	–	–
PLA/PBT	55.8	114.7	12.3	162.4 167.7	39.0	215.4 225.4	27.9
PBT	–	–	–	–	–	224.4	32.5
PLA/PPDI	58.3	113.4	30.8	162.7	36.1	–	–
PLA/PBT/PPDI	57.1	98.7	8.1	166.4	36.2	219.1	17.2
PBT/PPDI	–	–	–	–	–	214.4 220.7	24.4

stage are summarized in Table 3. The apparent degree of crystallinity (X_c) can be approximated using the following equation:

$$X_c\ (\%) = \frac{\Delta H_{m,i}}{\varphi_i\, \Delta H_{m,i}^{ideal}} \times 100, \tag{2}$$

where $\Delta H_{m,i}$ is the measured heat of fusion of PLA or PBT phases, φ_i is the weight fraction of PLA or PBT, and $\Delta H_{m,i}^{ideal}$ is the enthalpy of fusion for a crystal having infinite crystal thickness (93 J/g for PLLA [16, 17, 32], 142 J/g for PBT [25, 33, 34]).

The PLA added into PBT matrix decreased the X_c of a PBT phase by about 5% as PBT and PLA/PBT are compared. The X_c values of PLA phases in PLA/PPDI and PLA/PBT/PPDI were smaller than that in the PLA/PBT by about 3%, and the X_c values of PBT phases in PBT/PPDI and PLA/PBT/PPDI were also much smaller than that in the PLA/PBT as well as the pure PBT. Therefore, the chain extension of PPDI reduces the degree of perfection of crystals in the PLA or PBT phases because an increase in molecular weight decreases chain mobility [35]. Figure 6 shows the crystallization temperatures of the PLA/PBT and the PLA/PBT/PPDI at two different rates of 10 and 20°C/min during cooling and reheating stages. The crystallization peak of a PLA phase in the PLA/PBT/PPDI was also detected near 93°C at a rate of 10°C/min like the DSC result at a rate of 20°C/min during the cooling stage. Moreover, the crystallization temperatures of the PLA and PBT phases at a cooling rate of 10°C/min were higher than those at 20°C/min, and the cold crystallization temperatures of the PLA phases at a reheating rate of 10°C/min were lower than those at 20°C/min. Consequently, the onset temperatures of the crystallization of the PLA and PBT phases depend strongly on the variation rate of temperature.

The PLA/PBT blends were annealed at a specific temperature of 75°C for 30 min, and the crystallization behavior was measured by WAXD as shown in Fig. 7. The crystallized pure PLA exhibits a very strong reflection at $2\theta = 17.1°$

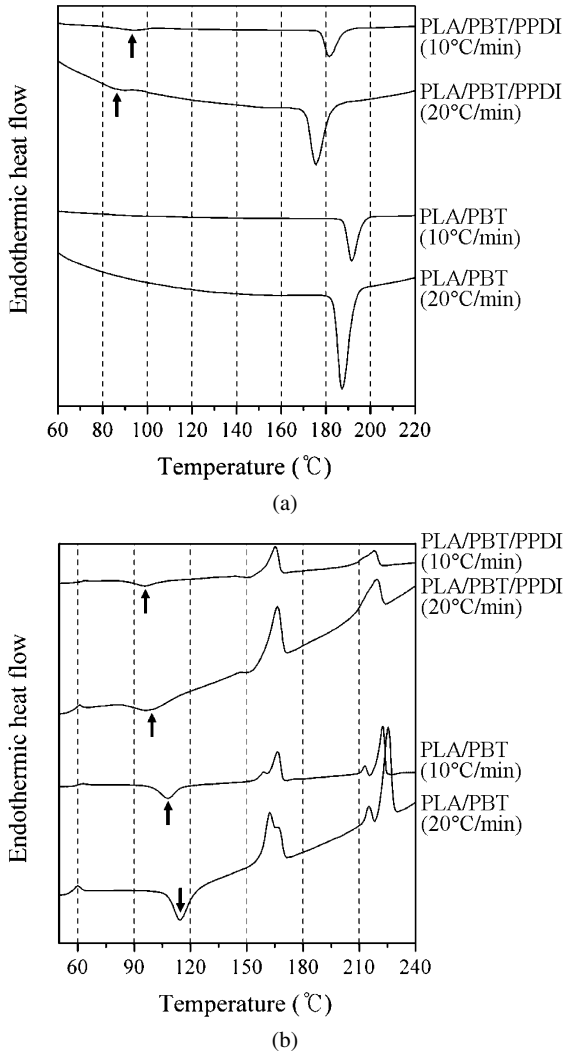

Figure 6. Comparison of the crystallization temperatures of PLA/PBT and PLA/PBT/PPDI at two different rates of 10 and 20°C/min during (a) a cooling stage and (b) a reheating stage.

due to diffraction from (200) and/or (110) planes, and another reflection peak occurs at $2\theta = 19.5°$ due to diffraction from (203) plane [5, 36]. This profile indicates that pure PLA crystals are typical orthorhombic crystals [37]. The crystallized pure PBT shows five strong diffraction peaks at 15.8°, 17.1°, 20.4°, 23.2° and 25.08° which correspond to the $(0\bar{1}1)$, (010), (011), (100) and $(1\bar{1}1)$ diffraction planes, respectively [38, 39].

The crystallization of the PLA phases did not happen in pure PLA and PLA/PPDI, whereas it occurred in PLA/PBT and PLA/PBT/PPDI whose crystallinity was 6.1% and 4.8%, respectively, in the same annealing conditions as

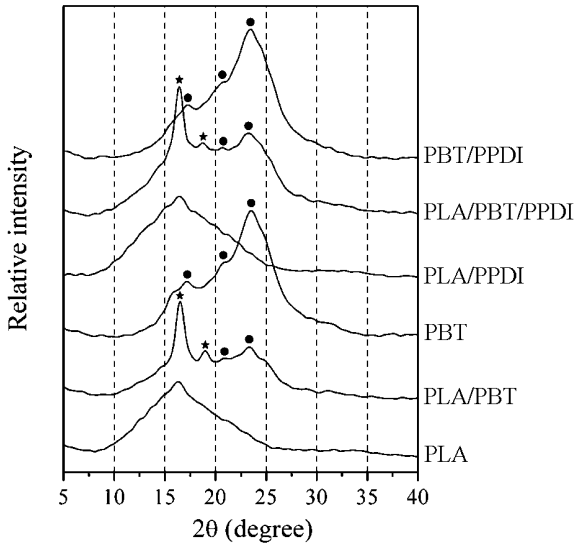

Figure 7. WAXD curves of the PLA/PBT blends annealed at 75°C for 30 min.

Table 4.
Degradation rates after 2 weeks and the properties related to the biodegradability of the PLA/PBT blends

Sample	Contact angle (°)	PLA phase	
		Crystallinity by WAXD (%)	Degradation rate after 2 weeks (wt%)
PLA	64.8 ± 0.6	0	0.36
PLA/PBT	63.4 ± 1.1	6.1	0.54
PBT	63.5 ± 0.8	–	–
PLA/PPDI	67.4 ± 0.4	0	0.36
PLA/PBT/PPDI	64.6 ± 1.3	4.8	0.39
PBT/PPDI	64.6 ± 0.4	–	–

shown in Table 4. Moreover, the creation of new peaks or the shift of peaks was not detected in the PLA/PBT and the PLA/PBT/PPDI. This indicates that the cocrystallization of both PLA and PBT molecules in the same crystalline region did not occur. The crystallization of each PLA and PBT phase progressed independently, and the crystallization-induced phase separation occurred to form pure phases separately [15].

3.4. Morphological Property

Figure 8 shows the SEM images of the fracture surface of PLA, PLA/PPDI, PLA/PBT, and PLA/PBT/PPDI specimens annealed at 75°C for 30 min in order to investigate the chain extension effects of PPDI on the morphology of PLA and

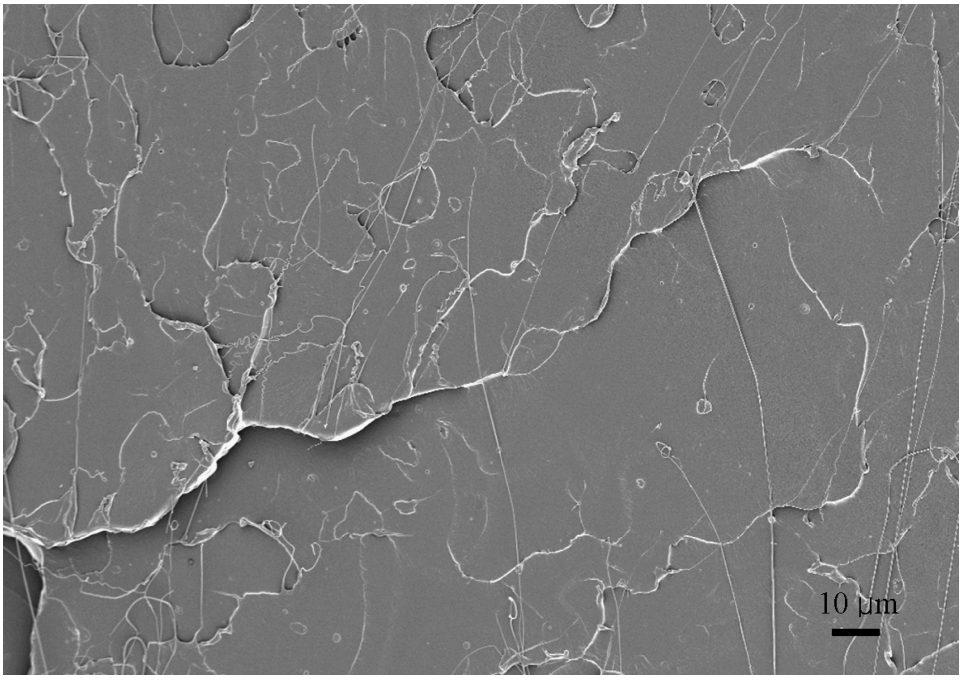

(a)

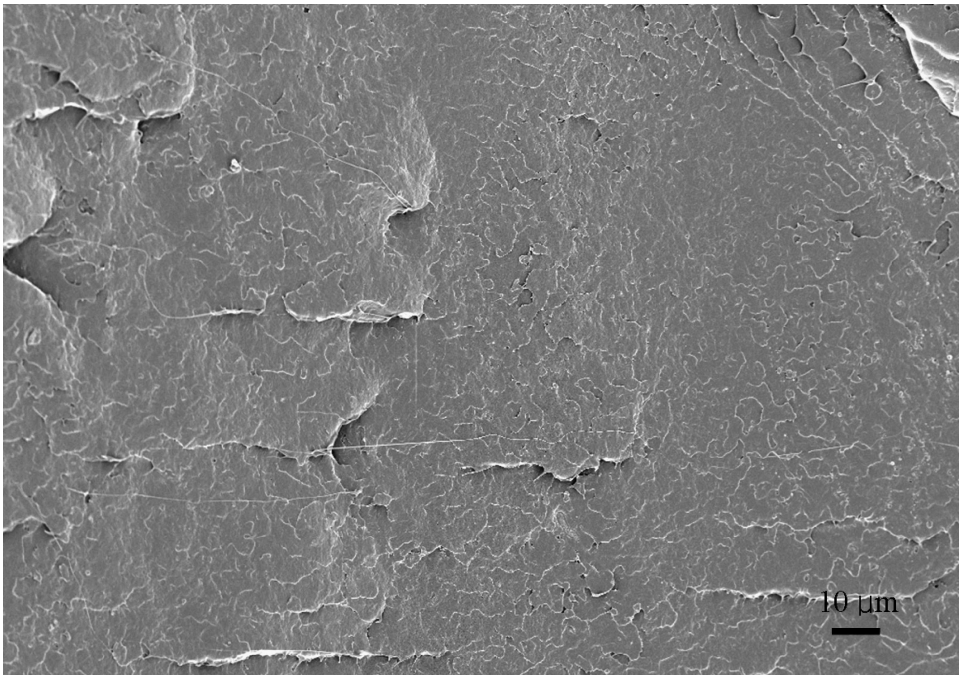

(b)

Figure 8. SEM images of the fracture surfaces of (a) PLA, (b) PLA/PPDI, (c) PLA/PBT and (d) PLA/PBT/PPDI specimens annealed at 75°C for 30 min.

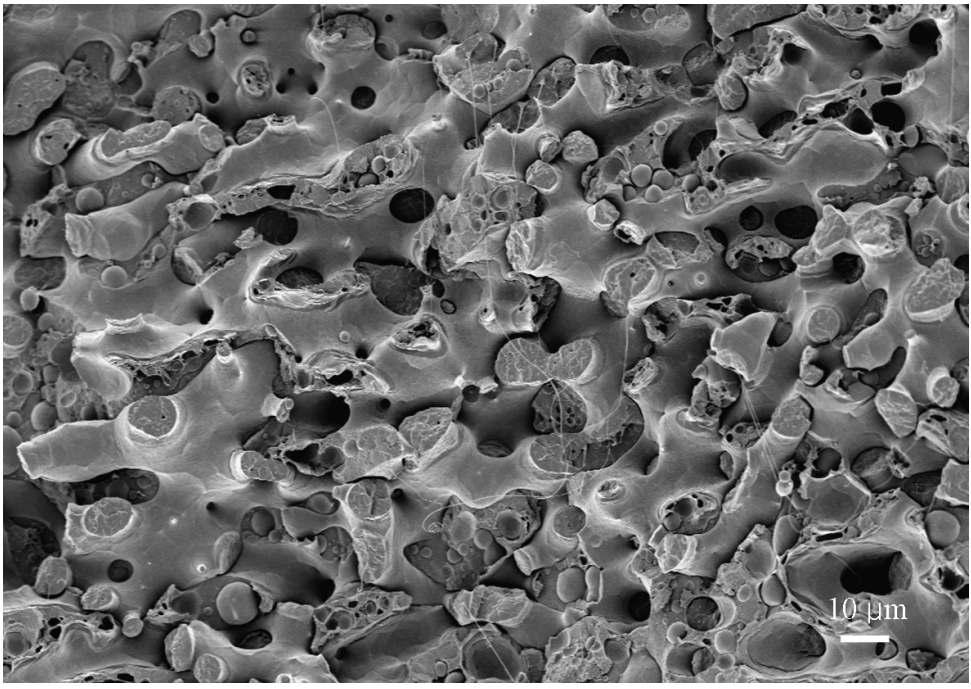

(c)

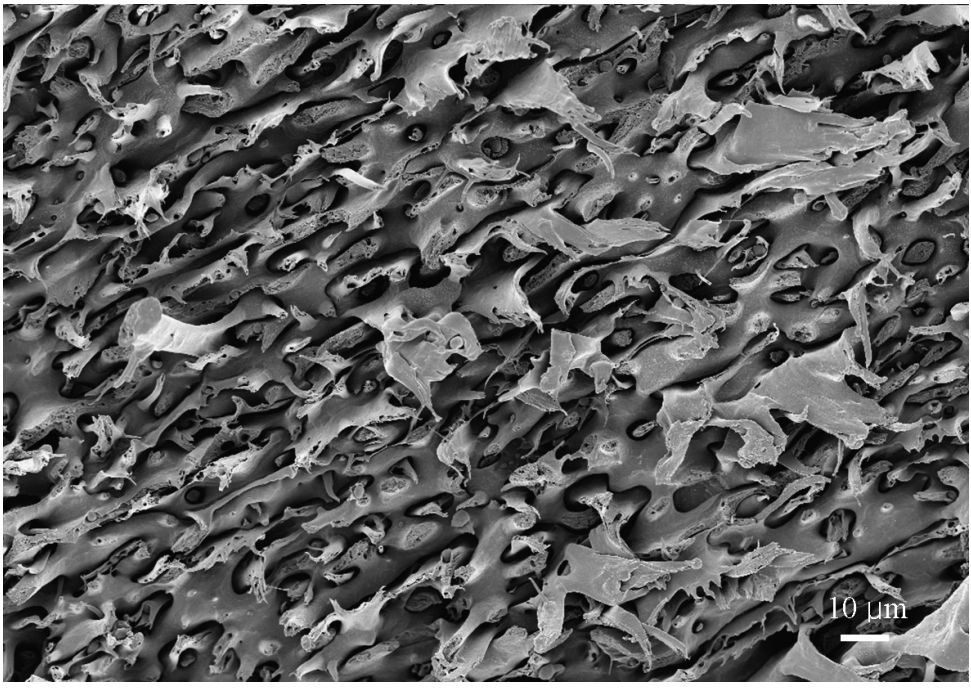

(d)

Figure 8. (Continued.)

PBT phases. The fracture surface of the PLA/PPDI was rougher than that of the pure PLA as shown in Fig. 8(a) and 8(b). It was also observed that the chain extension of PLA caused by the reaction with PPDI was generated uniformly. As two phases are shown in Fig. 8(c), it is noticed that many PBT granules were pulled out from the PLA matrix with many voids created by the fracture process because PBT is much more ductile than PLA. This result implies the poor interfacial adhesion between the PLA and PBT matrices and the typical morphology of incompatible polymer blends. In contrast, Fig. 8(d) shows that the PBT phases were torn off or elongated in the PLA matrix owing to the improved interfacial adhesion between the PLA and PBT phases through the chemical reaction with the PPDI.

3.5. Enzymatic Degradation

The degradation rates of PLA phases in the PLA/PBT blends annealed at 75°C for 30 min are shown in Fig. 9. The degradation rates of the PLA phases were calculated by using the following equation:

$$\text{Degradation rate (wt\%)} = \frac{w_{\text{original}} - w_{\text{degraded}}}{\varphi_i \, w_{\text{original}}} \times 100, \tag{3}$$

where w_{original} is the original weight of the specimens, w_{degraded} is the degraded weight of the specimens, and φ_i is the weight fraction of PLA phases. It was observed that the remaining weight of all specimens decreased almost linearly with elapsing time. The degradation rates of PLA/PBT and PLA/PBT/PPDI were faster than those of pure PLA and PLA/PPDI. It was more difficult for a PLA/PBT blend reacted with PPDI to be degraded than that without PPDI as the PLA/PBT and the PLA/PBT/PPDI were compared. The PBT phase was not degraded at all by the enzyme used in this study.

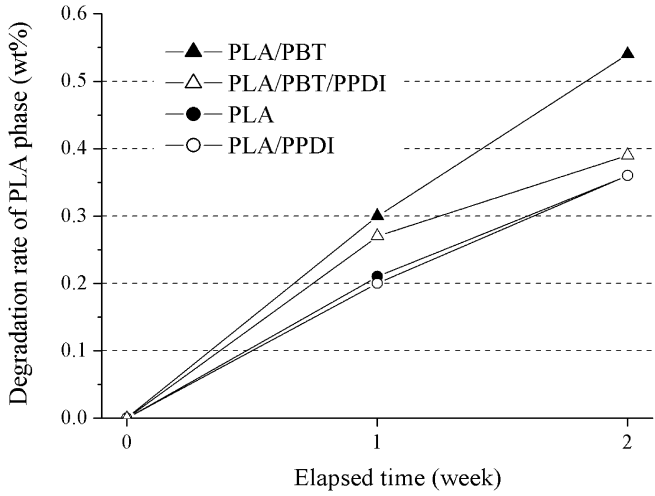

Figure 9. Degradation rates of PLA phases in the PLA/PBT blends annealed at 75°C for 30 min.

The degradation rates after 2 weeks and the properties related to the biodegradability of the PLA/PBT blends are listed in Table 4 to compare the effects of crystallinity, morphology, and hydrophilicity on the biodegradability of the PLA phases in the same condition. It is noticed that both PLA and PBT, which have similar contact angles, are similarly hydrophobic. According to the variation in contact angles before and after the reaction of PLA, PLA/PBT and PBT with PPDI, their average contact angles were slightly increased after the reaction. However, it is shown that all the samples are very similar in their hydrophilicity because their contact angles were almost the same.

It is known that the biodegradability of PLA decreases with an increase in the crystallinity because the amorphous phase undergoes hydrolysis preferentially [40]. But the crystallinity of the samples does not seem to influence the biodegradability of PLA phases in a PLA/PBT blending system. However, the phase separation between PLA and PBT in PLA/PBT blends can increase the interfacial area exposed to the hydrolysis of enzyme as shown in Fig. 8(c). In contrast, the improved interfacial adhesion between the PLA and PBT phases decreased the area which was exposed to the enzyme, resulting in decreasing the degradation rate of the PLA phase.

4. Conclusions

The rheological properties of PLA/PPDI and PBT/PPDI showed that the end groups of PLA and PBT molecules were extended by PPDI during the reaction extrusion. Blending PLA and PBT improved the crystallization rate of each phase but decreased the crystallinity of the PBT phase. When PLA, PBT and PPDI were reacted together, the crystallization rate of PLA was improved due to the synergy effect. Since the solidification time for the material is a function of the crystallization rate, the fast crystallization can shorten the cycle time of the injection molding. However, the crystallinity of both PLA and PBT phases was decreased by the chain extension of PPDI. The phase separation between PLA and PBT improved the biodegradability of PLA phases in the PLA/PBT blends, whereas the improved interfacial adhesion between PLA and PBT induced by the reaction with PPDI decreased the degradation rate of PLA. The decrease in biodegradability may enhance the long term durability of the PLA/PBT blends.

Acknowledgements

This study was supported by the Korea Science and Engineering Foundation (KOSEF) grant funded by the Korean government (MEST) (R11-2005-065) through the Intelligent Textile System Research Center (ITRC). The authors are grateful for the support.

References

1. T. Li, L.-S. Turng, S. Gong and K. Erlacher, Polylactide, nanoclay, and core–shell rubber composites, *Polym. Engng Sci.* **46**, 1419–1427 (2006).

2. B.-H. Li and M.-C. Yang, Improvement of thermal and mechanical properties of poly(L-lactic acid) with 4,4-methylene diphenyl diisocyanate, *Polym. Adv. Technol.* **17**, 439–443 (2006).
3. S. S. Ray, K. Yamada, M. Okamoto and K. Ueda, New polylactide-layered silicate nanocomposites. 2. Concurrent improvements of material properties, biodegradability and melt rheology, *Polymer* **44**, 857–866 (2003).
4. S. S. Ray, K. Yamada, M. Okamoto, A. Ogami and K. Ueda, New polylactide/layered silicate nanocomposites. 3. High-performance biodegradable materials, *Chem. Mater.* **15**, 1456–1465 (2003).
5. M. Okamoto, Biodegradable polymer/layered silicate nanocomposites: a review, *J. Ind. Engng Chem.* **10**, 1156–1181 (2004).
6. Q. Fang and M. A. Hanna, Rheological properties of amorphous and semicrystalline polylactic acid polymers, *Ind. Crop. Prod.* **10**, 47–53 (1999).
7. T. Semba, K. Kitagawa, U. S. Ishiaku, M. Kotaki and H. Hamada, Effect of compounding procedure on mechanical properties and dispersed phase morphology of poly(lactic acid)/polycaprolactone blends containing peroxide, *J. Appl. Polym. Sci.* **103**, 1066–1074 (2007).
8. N. Kawamoto, A. Sakai, T. Horikoshi, T. Urushihara and E. Tobita, Physical and mechanical properties of poly(L-lactic acid) nucleated by dibenzoylhydrazide compound, *J. Appl. Polym. Sci.* **103**, 244–250 (2007).
9. H. Tsuji and Y. Ikada, Properties and morphologies of poly(L-lactide): 1. Annealing condition effects on properties and morphologies of poly(L-lactide), *Polymer* **36**, 2709–2716 (1995).
10. B. J. Chisholm and J. G. Zimmer, Isothermal crystallization kinetics of commercially important polyalkylene terephthalates, *J. Appl. Polym. Sci.* **76**, 1296–1307 (2000).
11. G. Aravinthan and D. D. Kale, Blends of poly(ethylene terephthalate) and poly(butylene terephthalate), *J. Appl. Polym. Sci.* **98**, 75–82 (2005).
12. A. M. Gajria, V. Davé, R. A. Gross and S. P. McCarthy, Miscibility and biodegradability of blends of poly(lactic acid) and poly(vinyl acetate), *Polymer* **37**, 437–444 (1996).
13. L. Jiang, M. P. Wolcott and J. Zhang, Study of biodegradable polylactide/poly(butylene adipate-co-terephthalate) blends, *Biomacromolecules* **7**, 199–207 (2006).
14. Y. Hu, M. Rogunova, V. Topolkaraev, A. Hiltner and E. Baer, Aging of poly(lactide)/poly(ethylene glycol) blends. Part 1. Poly(lactide) with low stereoregularity, *Polymer* **44**, 5701–5710 (2003).
15. J. W. Park and S. S. Im, Phase behavior and morphology in blends of poly(L-lactic acid) and poly(butylene succinate), *J. Appl. Polym. Sci.* **86**, 647–655 (2002).
16. M. Peesan, P. Supaphol and R. Rujiravanit, Preparation and characterization of hexanoyl chitosan/polylactide blend films, *Carbohydr. Polym.* **60**, 343–350 (2005).
17. K. S. Anderson, S. H. Lim and M. A. Hillmyer, Toughening of polylactide by melt blending with linear low-density polyethylene, *J. Appl. Polym. Sci.* **89**, 3757–3768 (2003).
18. C. Nakafuku and M. Sakoda, Melting and crystallization of poly(L-lactic acid) and poly(ethylene oxide) binary mixture, *Polym. J.* **25**, 909–917 (1993).
19. L. Zhang, S. H. Goh and S. Y. Lee, Miscibility and crystallization behaviour of poly(L-lactide)/poly(p-vinylphenol) blends, *Polymer* **39**, 4841–4847 (1998).
20. G. Zhang, J. Zhang, X. Zhou and D. Shen, Miscibility and phase structure of binary blends of polylactide and poly(vinylpyrrolidone), *J. Appl. Polym. Sci.* **88**, 973–979 (2003).
21. T. Shirahase, Y. Komatsu, Y. Tominaga, S. Asai and M. Sumita, Miscibility and hydrolytic degradation in alkaline solution of poly(L-lactide) and poly(methyl methacrylate) blends, *Polymer* **47**, 4839–4844 (2006).
22. H. Wang, X. Sun and P. Seib, Strengthening blends of poly(lactic acid) and starch with methylenediphenyl diisocyanate, *J. Appl. Polym. Sci.* **82**, 1761–1767 (2001).

23. S.-H. Lee and S. Wang, Biodegradable polymers/bamboo fiber biocomposite with bio-based coupling agent, *Composites Part A* **37**, 80–91 (2006).
24. L. E. Alexander, *X-ray Diffraction Methods in Polymer Science*. Wiley-Interscience, New York, USA (1969).
25. E. S. Kumar, S. B. Yadaw, K. N. Pandey and C. K. Das, Ternary blends of acrylic rubber, poly(butylene terephthalate), and liquid crystalline polymer: influence of interactions on thermal and dynamic mechanical properties, *J. Appl. Polym. Sci.* **100**, 3904–3912 (2006).
26. S. Rabiej, B. Ostrowska-Gumkowska and A. Wlochowicz, Investigations of the crystallinity of PA-6/SPS blends by X-ray diffraction and DSC methods, *Eur. Polym. J.* **33**, 1031–1039 (1997).
27. Y. Yu and K.-J. Choi, Crystallization in blends of poly(ethylene terephthalate) and poly(butylene terephthalate), *Polym. Engng Sci.* **37**, 91–95 (1997).
28. H. A. Barnes, *A Handbook of Elementary Rheology*. Institute of Non-Newtonian Fluid Mechanics, University of Wales, UK (2000).
29. W. Zhong, J. Ge, Z. Gu, W. Li, X. Chen, Y. Zang and Y. Yang, Study on biodegradable polymer materials based on poly-(lactic acid). I. Chain extending of low molecular weight poly(lactic acid) with methylenediphenyl diisocyanate, *J. Appl. Polym. Sci.* **74**, 2546–2551 (1999).
30. S. I. Woo, B. O. Kim, H. S. Jun and H. N. Chang, Polymerization of aqueous lactic acid to prepare high molecular weight poly(lactic acid) by chain-extending with hexamethylene diisocyanate, *Polym. Bull.* **35**, 415–421 (1995).
31. J.-R. Sarasua, R. E. Prud'homme, M. Wisniewski, A. L. Borgne and N. Spassky, Crystallization and melting behavior of polylactides, *Macromolecules* **31**, 3895–3905 (1998).
32. E. W. Fischer, H. J. Sterzel and G. Wegner, Investigation of the structure of solution grown crystals of lactide copolymers by means of chemical reactions, *Kolloid-Z. u. Z. Polymere* **251**, 980–990 (1973).
33. K.-H. Illers, Heat of fusion and specific volume of poly(ethylene terephthalate) and poly(butylene terephthalate), *Colloid Polym. Sci.* **258**, 117–124 (1980).
34. W.-B. Liau, S.-H. Tung, W.-C. Lai and L.-Y. Yang, Studies on blends of binary crystalline polymers: miscibility and crystallization behavior in PBT/PAr(I27-T73), *Polymer* **47**, 8380–8388 (2006).
35. G. Perego, G. D. Cella and C. Bastioli, Effect of molecular weight and crystallinity on poly(lactic acid) mechanical properties, *J. Appl. Polym. Sci.* **59**, 37–43 (1996).
36. J. Y. Nam, M. Okamoto, H. Okamoto, M. Nakano, A. Usuki and M. Matsuda, Morphology and crystallization kinetics in a mixture of low-molecular weight aliphatic amide and polylactide, *Polymer* **47**, 1340–1347 (2006).
37. L. Cartier, T. Okihara, Y. Ikada, H. Tsuji, J. Puiggali and B. Lotz, Epitaxial crystallization and crystalline polymorphism of polylactides, *Polymer* **41**, 8909–8919 (2000).
38. H. Zou, J. Jiang, S. Yang and G. Li, The composition, sequence analysis and crystallization characterization of poly(trimethylene-co-butylene terephthalate) copolymer, *J. Macromol. Sci. Phys.* **45**, 581–592 (2006).
39. R. K. Y. Li, S. C. Tjong and X. L. Xie, The structure and physical properties of *in situ* composites based on semiflexible thermotropic liquid crystalline copolyesteramide and poly(butylene terephthalate), *J. Polym. Sci. Part B: Polym. Phys.* **38**, 403–414 (2000).
40. H. Urayama, T. Kanamori and Y. Kimura, Properties and biodegradability of polymer blends of poly(L-lactide)s with different optical purity of the lactate units, *Macromol. Mater. Engng* **287**, 116–121 (2002).